Tree Physiology 36, 942–953
doi:10.1093/treephys/tpw060

Research paper

Site-specific water-use strategies of mountain pine and larch to cope with recent climate change

Olga V. Churakova (Sidorova)[1,2,3,6], Matthias Saurer[2], Marina V. Bryukhanova[4,5], Rolf T.W. Siegwolf[2] and Christof Bigler[1]

[1]Department of Environmental Systems Science, Forest Ecology, Institute of Terrestrial Ecosystems, ETH Zürich, Universitätstrasse 16, 8092 Zürich, Switzerland; [2]Paul Scherrer Institute, 5232 Villigen, PSI, Switzerland; [3]Dendrolab.ch, Institute of Geological Sciences, University of Bern, Balzerstrasse 1+3, 3012 Bern, Switzerland; [4]V.N. Sukachev Institute of Forest, SB RAS, 660036 Krasnoyarsk, Akademgorodok, Russia; [5]Siberian Federal University, 79 Svobodny pr., 660041 Krasnoyarsk, Russia; [6]Corresponding author (olga.churakova@dendrolab.ch)

Received February 5, 2016; accepted June 9, 2016; handling Editor Lucas Cernusak

We aim to achieve a mechanistic understanding of the eco-physiological processes in *Larix decidua* and *Pinus mugo* var. *uncinata* growing on north- and south-facing aspects in the Swiss National Park in order to distinguish the short- and long-term effects of a changing climate. To strengthen the interpretation of the $\delta^{18}O$ signal in tree rings and its coherence with the main factors and processes driving evaporative $\delta^{18}O$ needle water enrichment, we analyzed the $\delta^{18}O$ in needle, xylem and soil water over the growing season in 2013 and applied the mechanistic Craig–Gordon model (1965) for the short-term responses. We found that $\delta^{18}O$ needle water strongly reflected the variability of relative humidity mainly for larch, while only $\delta^{18}O$ in pine xylem water showed a strong link to $\delta^{18}O$ in precipitation. Larger differences in offsets between modeled and measured $\delta^{18}O$ needle water for both species from the south-facing aspects were detected, which could be explained by the high transpiration rates. Different soil water and needle water responses for the two species indicate different water-use strategies, further modulated by the site conditions. To reveal the long-term physiological response of the studied trees to recent and past climate changes, we analyzed $\delta^{13}C$ and $\delta^{18}O$ in wood chronologies from 1900 to 2013. Summer temperatures as well as summer and annual amount of precipitations are important factors for growth of both studied species from both aspects. However, mountain pine trees reduced sensitivity to temperature changes, while precipitation changes come to play an important role for the period from 1980 to 2013. Intrinsic water-use efficiency (WUEi) calculated for larch trees since the 1990s reached a saturation point at elevated CO_2. Divergent trends between pine WUEi and $\delta^{18}O$ are most likely indicative of a decline of mountain pine trees and are also reflected in decoupling mechanisms in the isotope signals between needles and tree-rings.

Keywords: climate, $\delta^{13}C$ and $\delta^{18}O$ in wood, $\delta^{18}O$ in needle, soil and xylem water, intrinsic water-use efficiency, pine decline, tree-ring width.

Introduction

In the last 20 to 30 years forests have been affected in many regions by water deficits during droughts due to increasing temperatures and decreased precipitation (Allen et al. 2010, Klein 2015). Climate models predict that drought frequency will continue to increase during the twenty-first century and beyond (CH 2011, Pachauri et al. 2014). In the future, increasing temperatures will enhance the evaporative demand and water loss from plants and may reduce productivity and carbon sequestration in many forest ecosystems (Sidorova et al. 2009, Anderegg et al. 2012). To project changes in forest ecosystems, we have to deepen our understanding of the underlying mechanisms by which trees can survive with decreasing precipitation, which can enhance and accelerate tree mortality and forest decline (Sala et al. 2010, Klein 2015).

Trees growing at high altitude are particularly sensitive to climatic and environmental changes (Körner 2012). To understand

long-term changes on the tree level, analysis of seasonal variability of tree physiological responses is needed. Climatic parameters like temperature, water availability, air humidity and ambient CO_2 (c_a) influence photosynthetic CO_2 assimilation and water balance, which is reflected in the isotopic carbon and oxygen isotope ratios of the plant organic matter, yielding a specific isotope pattern in the wood of tree rings. Under warm and dry conditions trees respond to limited water resources by reducing stomatal conductance (g_s), resulting in a diminished CO_2 uptake and biomass production, and also in reduced intercellular CO_2 concentration (c_i). The latter leads to reduced ^{13}C discrimination (Farquhar et al. 1989) and increased $\delta^{18}O$ values (Farquhar and Lloyd 1993). $\delta^{18}O$ values in tree rings reflect the condensation temperature during rain formation, which represents the source water for trees' and leaves' water enrichment (Craig 1961, McCarroll and Loader 2004). Enrichment in $\delta^{18}O$ occurs in the needles or leaves during transpiration, which may be enhanced under drought conditions (Yakir 1998). A mixed seasonal signal of water source and water enrichment in leaves is finally stored in the wood and cellulose of tree rings (Saurer et al. 1997, Roden et al. 2000).

In our study, we focus on mountain pine and larch as two key species in high-altitude forests. Several studies reported declines of mountain pine trees in north Germany, Poland, the Pyrenees, the Carpathians, the northern Apennines and the Balkan Peninsula (Solar 2013), and in the Swiss National Park (SNP) (Brang 1988, Cherubini et al. 2002, Bendel et al. 2006*a*, 2006*b*). European larch (*Larix decidua* Mill.) growing near the tree line is better adapted to cold climate conditions than mountain pine (Körner 2012) and may reach life spans of more than 500 years. Such long-living larch trees allow us to reveal physiological responses of trees to climatic and environmental changes far back into the past and provide insight into the magnitude and forcing mechanisms of the recent climatic changes. In this study, we investigate and compare the physiological responses of mountain pine and larch growing on different aspects under different microclimatic conditions to recent and past climatic changes. To detect physiological responses of mountain pine and larch trees to weather changes and to understand the origin of the water source (i.e., soil depth) used by larch and mountain pine trees from south- and north-facing aspects we analyzed $\delta^{18}O$ soil ($\delta^{18}O_{Soil}$), xylem ($\delta^{18}O_{Xyl}$) and needle ($\delta^{18}O_{Needle}$) water as short-term indicators. To reveal long-term changes in water use for these two species growing on two different aspects and their responses to recent and past climatic and environmental changes we analyzed $\delta^{13}C$ and $\delta^{18}O$ in wood for the last 100 years.

In our study we addressed the following research questions:

(i) Are there differences in the seasonal $\delta^{18}O$ courses in $\delta^{18}O_{Needle}$, $\delta^{18}O_{Xyl}$ and $\delta^{18}O_{Soil}$ water (source water) between larch and mountain pine trees growing on south- and north-facing aspects?

(ii) Which of the investigated climatic factors (temperature, air humidity or water availability) are predominantly reflected in $\delta^{18}O$ of wood in larch and mountain pine trees in the long term?

(iii) Do mountain pine and larch trees show different water-use efficiency (WUE) strategies under recent climatic changes?

Materials and methods

Study site and sampling

The study site is situated at 1959–1964 m above sea level (a.s.l.) at Champlönch in the SNP, Switzerland (46°N, 10°E). Around 28% of the SNP is forested, 21% is alpine grasslands and 51% unproductive terrain. Mountain pine (*Pinus mugo* subsp. *uncinata*) and dwarf mountain pine (*Pinus mugo* subsp. *mugo*) predominantly grow on limestone in the SNP, and cover ~73% of the forests in the SNP. *Pinus mugo* subsp. *uncinata* and *P. mugo* subsp. *mugo* are light-demanding species, which do not exhibit particular soil preferences but need sufficient water availability (Bendel et al. 2006*a*). Forests with European larch and Swiss stone pine (*Pinus cembra*) cover ~11% of the forests in the SNP.

The study site is characterized by a continental climate. According to the climate station Buffalora (~11.6 km from study site; 1968 m a.s.l., 10° 16′ E and 46° 38′N) the average winter temperature is −9.2 °C and summer temperature is +9.5 °C (monthly averages from 1917 to 2013). Since the 1990s mean annual and spring temperatures increased by 0.5 and 1.0 °C, respectively, while the average summer temperature increased by 0.6 °C. The annual sum of precipitation is 910 mm (period 1917 to 2013). Since the 1990s annual precipitation decreased by 88.9 mm compared with the mean value of 931.2 mm from 1917 to 1989.

We selected two contrasting aspects at Champlönch, a south-facing sunny slope at 1964 m a.s.l. and a north-facing shady slope at 1959 m a.s.l. The inclination at the south-facing aspect is 35% compared with 20% at the north-facing aspect. At the north-facing aspect the soil tends to be cooler and moister, and is covered by denser ground vegetation compared with the south-facing aspect.

On each aspect, four dominant trees for larch and mountain pine were cored twice per tree for stable $\delta^{13}C$ and $\delta^{18}O$ isotope analysis. In October 2013, extra tree cores were collected from 12 additional trees per species and aspect for the construction of tree-ring width index (TRWI) chronologies.

During the growing season of 2013 we collected samples from needles and twigs from larch and mountain pine twice per month on sunny days. $\delta^{18}O$ isotope analysis was performed for water, extracted from the old needles of the previous growth season of 2012 and from the new needles of the current growth season of 2013 for mountain pine trees from the south- and north- facing aspects (PS and PN, respectively). The growing

season of 2013 started relatively late. Needles from larch trees growing on the south- facing aspect (LS) were longer at the first sampling date on 25 May 2013 compared with the north- facing aspect (LN), while no fresh needles from mountain pine trees were visible.

Precipitation was collected twice per month in a rain collector with a small table tennis ball on the top of the funnel pipe to avoid changes of $\delta^{18}O$ in precipitation water ($\delta^{18}O_{Pr}$) as a result of evaporation. Soil samples were collected close to each tree, with one sample each from the uphill and downhill side. Because of the rocky and shallow soil we could only access the topmost 10 cm soil layer. Based on the results from Treydte et al. (2014), who showed that variation of the $\delta^{18}O$ in soil during the season is relatively low, soil samples at our study sites were collected once per month during the study season of 2013. All samples were immediately stored in airtight glass vials and frozen at –21 °C before extracting the soil water in the laboratory for the isotopic analysis.

Tree-ring analysis

Each 12 increment cores from larch and mountain pine were glued on core mounts and polished or cut, respectively, for visualization of tree cells (Cook and Kairiukstis 1990). Then tree rings were counted and measured using a LINTAB 5 measurement bench (Rinntech, Heidelberg, Germany) under a stereomicroscope (Leica MZ6). The cross-dating procedure to determine the exact formation year of each tree ring and for building individual raw tree-ring width chronologies was carried out using TSAPWin (Rinntech) and the software COFECHA (Holmes 1983). To remove the age trend for each raw tree-ring width series we standardized each series by applying a negative exponential or linear function (Holmes 1983). For the further analysis residual tree-ring index chronologies were used.

$\delta^{13}C$ and $\delta^{18}O$ analyses

Two increment cores from each tree were sampled for the stable isotope analysis from the same trees used for tree-ring analysis. Resins from the samples were extracted with a Soxhlet apparatus with a 1:1 ethanol–methanol mixture during 48 h. Tree cores were then washed with distilled water for 24 h and air dried at room temperature. For a better visualization of the tree rings the surface of the tree cores were slightly cut by hand without polishing or application of powder, to avoid cross contamination between the tree rings, which must be considered for the $\delta^{13}C$ and $\delta^{18}O$ stable isotope analysis in wood. The tree rings were measured and cross-dated against the dated tree-ring series, which were used for tree-ring analyses. For each tree, each annual ring (including early and late wood) was split separately using a scalpel. Wood samples were then milled to a fine powder and packed into silver capsules. Simultaneous measurements for $\delta^{13}C$ and $\delta^{18}O$ of wood samples were performed with a vario PYRO cube (Elementar, Hanau, Germany) via thermic decomposition at 1450 °C and conversion to CO under O_2 exclusion in helium (Woodley et al. 2012). This system was linked to an isotope-ratio mass spectrometer (IRMS) (Delta plus XP, Thermo Finnigan, Bremen, Germany). In this work, we analyzed only whole wood samples because the small tree rings provided only little material and previous work showed that wood samples could capture climatic signals as well as cellulose (Sidorova et al. 2008).

Water extraction

The water extraction was carried out using a cryogenic water extraction line. Airtight glass vials with frozen needle, soil and twig samples were put in a water bath at 80 °C and connected to glass U-tubes, which were submerged in liquid nitrogen (LN_2). This line was under a vacuum of 0.03 hPa during 2 h and the evaporating water was trapped in the LN_2 cooled glass U-tubes. Then, $\delta^{18}O$ of the extracted water was analyzed via a High Temperature Combustion Elemental Analyzer (TC/EA, Thermo Finnigan) and an IRMS (Delta plus XP, Thermo Finnigan). The values were expressed in the delta notation referenced to Vienna Standard Mean Ocean Water (VSMOW).

Application of the Craig–Gordon model to tree organic matter

Our measurements were compared with the Craig–Gordon model results to obtain a mechanistic understanding of the main factors driving $\delta^{18}O_{Needle}$ water evaporative enrichment in two different species growing on two different aspects. The isotopic composition of $\delta^{18}O_{Needle}$ can be calculated using the Craig–Gordon leaf water enrichment equation (Craig and Gordon 1965, Dongmann et al. 1974):

$$\delta^{18}O_{Needle} = \delta^{18}O_s + \varepsilon_e + \varepsilon_k + (\delta^{18}O_{Vapor} - \delta^{18}O_s - \varepsilon_k)\, e_a/e_i, \quad (1)$$

where $\delta^{18}O_s$ is the isotope ratio of the mixture of soil and precipitation water used by trees, ε_e is the equilibrium fractionation factor accounting for the phase change from liquid to water vapor, ε_k is the kinetic fractionation due to diffusion of vapor into unsaturated air, $\delta^{18}O_{Vapor}$ is the isotopic composition of atmospheric water vapor and e_a/e_i is the ratio of external to needle internal water vapor pressures. Since ε_e is temperature dependent it needs to be corrected according to Bottinga and Craig (1968)

$$\varepsilon_e(‰) = 2.664 - 3/206\,(10^3/T_l) + 1/534\,(10^6/T_l^2), \quad (2)$$

where T_l is the needle temperature in Kelvin (K). Conifer needle temperature may be considered equal to air temperature (Barbour et al. 2002).

The isotopic composition of water vapor in the air $\delta^{18}O_{Vapor}$ can be estimated as the difference between $\delta^{18}O_s$ and ε_e, assuming that water vapor is in isotopic equilibrium with soil water (Förstel and Hützen 1983, Treydte et al. 2014). In general, Eq. (1) captures changes in leaf $\delta^{18}O$ quite well (Roden

and Ehleringer 1999), but this simple model may sometimes overestimate the real leaf enrichment, particularly when transpiration rates are high due to the Péclet effect (Farquhar and Lloyd 1993). The Péclet effect considers that the maximal enrichment according to the Craig–Gordon model is only reached at the evaporating surfaces, while the average needle water is diluted by replenishment of the transpired water with non-enriched xylem water from the roots.

Weather and tree-ring parameters

To relate the tree responses to seasonal weather variabilities we used hourly data for temperature, relative humidity (RH), vapor pressure deficit in the air (VPD) and reference evapotranspiration (RE), while in the longer-term we used annual (January–December), and average spring (March–May) and summer (June–August) air temperatures, the sums of precipitation for the same months for the period from 1917 to 2013, VPD for the period from 1959 to 2013, as well as RH and sunshine duration for the period from 2000 to 2013 from the Buffalora weather station. Based on available monthly temperature and precipitation data a drought index (DRI) was calculated as DRI = *P*-PET, with *P* equal to the monthly precipitation amount and PET equal to the monthly sum of estimated potential evapotranspiration as a function of monthly mean temperatures and geographical latitude following the formulation of Thornthwaite (1948).

Intrinsic water-use efficiency

$\delta^{13}C$ in plant organic tissue is related to the ratio of photosynthesis (A) to stomatal conductance (g_s), which is defined as carbon gain per maximum potential water loss and defined as intrinsic water-use efficiency (WUEi) (Farquhar and Sharkey 1982, Saurer et al. 2014).

$$\mathrm{WUEi} = A/g_s = (c_a - c_i)/1.6, \quad (3)$$

where c_a is the ambient CO_2 concentration, c_i the intercellular CO_2 concentration in the substomatal cavities and 1.6 is the ratio of diffusivities of water and CO_2 in the air.

Results

Seasonal variation of $\delta^{18}O$ in xylem, needle and soil water

Linear regression models were calculated for larch and pine from the south- (LS, PS) and north-facing (LN, PN) aspects with $\delta^{18}O$ in precipitation ($\delta^{18}O_{Pr}$) collected from our study site (Figure 1a and b, Table 1), VPD (Figure 1c and d) and RH (Figure 1e and f; Table 1).

Pearson's correlation analysis showed that VPD has a positive significant association with $\delta^{18}O_{Xyl}$ water for PS and PN (Figure 1d), while the influence was negative for LS and no significant influence of VPD for LN was found (Figure 1c). $\delta^{18}O_{Xyl}$ water was also significantly related to $\delta^{18}O_{Pr}$ for pine (Figure 1b) but not for larch (Figure 1a), while $\delta^{18}O_{Needle}$ water for LN was significantly correlated with RH only (Figure 1e). Furthermore, significant correlations between $\delta^{18}O_{Soil}$ water and RE (measured at the Buffalora weather station) were found for pine from both aspects (Table 1).

To test our $\delta^{18}O$ data for processes of evaporative $\delta^{18}O$ water enrichment we applied the mechanistic Craig–Gordon model (Eq. 1; Figure 2a and b). We computed mean $\delta^{18}O_{Soil}$ water from both aspects, using the measured data and extrapolated the soil data (average between two sampling dates) over the study season. A higher coherence between measured and modeled $\delta^{18}O_{Needle}$ water was found for larch (Figure 2a) compared with pine (Figure 2b). Yet, the model generally overestimated the needle enrichment for both species, resulting in large offsets (differences) between measured and modeled values, particularly for the south-facing aspect (Figure 2c).

Long-term variability

Tree-ring width chronologies Tree-ring width chronologies were built based on 12 tree cores from each species and each aspect. Average diameter at breast height (DBH) and average age of larch and pine trees was lower at the south-facing aspect (DBH = 35.5 cm and DBH = 21.6 cm; 193 and 185 years, respectively) compared with the north-facing aspect (DBH = 41.3 cm and DBH = 26.6 cm; 247 and 239 years, respectively). Correlation coefficients between individual cross-dated series for larch was higher than 0.62 and for pine higher than 0.49.

The LN and PN TRWI chronologies were constructed for the period from 1614 to 2013 and from 1729 to 2013, respectively. The chronologies on the southern aspect were shorter for both species: for larch from 1686 to 2013 and for pine from 1813 to 2013. The expressed population signal (EPS) (Wigley et al. 1984) was equal to or higher than 0.85, indicating a common signal between tree-ring series in year-to-year variations.

The TRWI showed a similar high-frequency pattern among sites (Figure 3a and b; Table 2) and were compared with the stable carbon and oxygen chronologies for larch and pine for both aspects for the common period from 1900 to 2013 only (Figure 3c–f).

$\delta^{13}C$ and $\delta^{18}O$ in wood The correlations between $\delta^{13}C$ and $\delta^{18}O$ chronologies were significant for LS, LN, PS and PN, but were higher for LS and LN compared with PS and PN. The highest correlations were found between LS and LN TRWI chronologies (Table 2).

For $\delta^{13}C$ we found large differences between PS and PN (Figure 3d and h) compared with LS and LN (Figure 3c and g). Surprisingly, the $\delta^{13}C$ for the LN chronology was, in general, more enriched in isotopic values compared with LS, while the opposite was the case for PN and PS. Especially, higher $\delta^{13}C$ values were found for LN during recent decades, which indicates

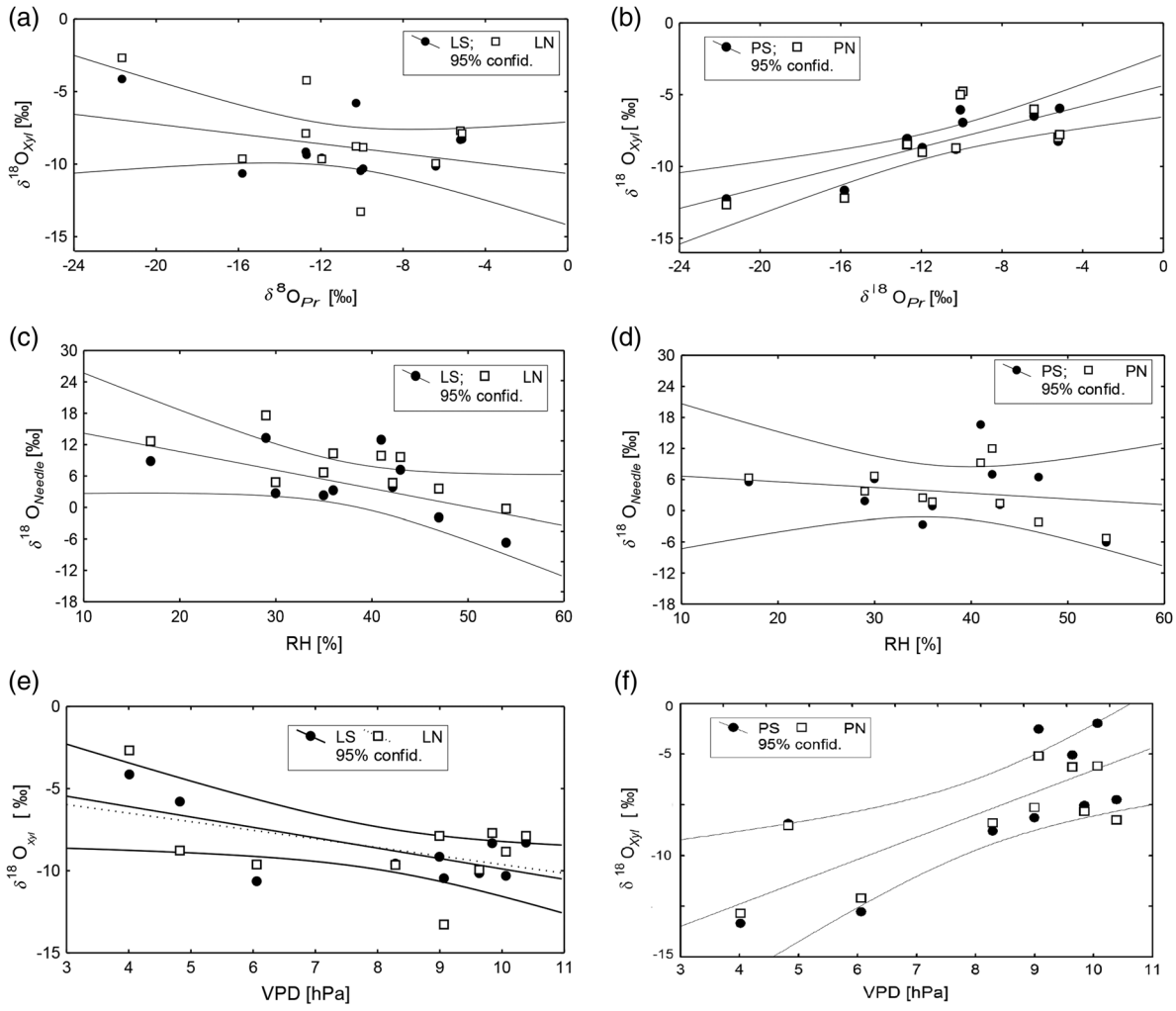

Figure 1. Scatter plots of (a and b) $\delta^{18}O$ xylem water ($\delta^{18}O_{Xyl}$) and $\delta^{18}O$ in precipitation water ($\delta^{18}O_{Pr}$); (c and d) $\delta^{18}O$ needle water ($\delta^{18}O_{Needle}$) and relative humidity (RH); (e and f) $\delta^{18}O$ xylem water ($\delta^{18}O_{Xyl}$) and VPD. The panels on the left show observations of larch on the south- and north- facing aspects (LS and LN), while the panels on the right show mountain pine on the south- and north- facing aspects (PS and PN). Regression lines and 95% confidence intervals are indicated.

a development of water shortage for larch trees at the north-facing aspect. The $\delta^{18}O$ values were more enriched for trees on the south- than on the north-facing aspect, resulting in positive deviations for both species (Figure 3g and h). From 1900 to 1980, the $\delta^{18}O$ larch chronologies showed a difference of up to 2.5‰ between the aspects followed by stronger similarity (Figure 3e). In contrast, the $\delta^{18}O$ pine chronology (Figure 3f) showed a smaller difference between PS and PN and a high coherence until 2000, after 2000 $\delta^{18}O$ of PS showed higher needle water enrichment compared with PN.

Response of larch and pine to climate change Pearson's correlation coefficients were calculated between TRWI, $\delta^{13}C$ and $\delta^{18}O$ in wood vs monthly temperature and precipitation from September previous year to August current year, and DRI for the period from 1917 to 2013. The analyzed period was divided into two sub-periods from 1917 to 1980 and from 1980 to 2013 to reveal the stability of the driving factors of tree growth in the long-term. We found that temperatures of June, July and August, precipitations of May, July, August and annual sums of precipitations, and DRI of May, July and August have the most significant influence on tree-ring parameters (Table 3).

We found a negative correlation of DRI of May with TRWI from LS and LN, while a positive correlation resulted with TRWI from PS and PN for the period from 1917 to 1980 (Table 3). The correlation between DRI of May and TRWI from PS remained positive and significant for the period from 1917 to 2013, which was not the case for TRWI from LS and LN.

$\delta^{13}C$ from LS and LN correlated negatively with DRI of July for all studied periods, while for $\delta^{13}C$ from PS a negative correlation was found for the period from 1917 to 1980 only.

The positive significant correlation coefficients remained stable over time between $\delta^{13}C$ from LN and July temperature.

Table 1. Pearson correlation coefficients between $\delta^{18}O$ in xylem ($\delta^{18}O_{Xyl}$), $\delta^{18}O$ in needle ($\delta^{18}O_{Needle}$) water from larch on south- and north-facing aspects (LS and LN) and pine from south- and north-facing aspects (PS and PN), as well as $\delta^{18}O_{Soil}$ water vs $\delta^{18}O$ in precipitation ($\delta^{18}O_{Pr}$), relative air humidity (RH), reference evapotranspiration (RE) and vapor pressure deficit in the air (VPD). Significant values are in bold, $P < 0.05$.

Parameter	Species/aspect	$\delta^{18}O_{Xyl}$	$\delta^{18}O_{Needle}$	$\delta^{18}O_{Soil}$
$\delta^{18}O_{Pr}$	LS	0.27	0.25	**0.89**
	LN	0.51	0.45	**0.66**
	PS	**0.83**	–0.30	**0.73**
	PN	**0.72**	–0.49	0.42
RH	LS	–0.19	–0.59	–0.24
	LN	0.47	**–0.69**	–0.46
	PS	0.07	–0.18	**–0.62**
	PN	0.04	–0.47	**–0.75**
RE	LS	–0.26	0.54	–0.45
	LN	–0.58	0.53	**–0.77**
	PS	0.16	0.42	**–0.79**
	PN	0.39	0.08	**–0.98**
VPD	LS	**–0.67**	0.28	0.61
	LN	–0.46	0.29	0.43
	PS	**0.76**	–0.02	0.42
	PN	**0.76**	–0.31	0.09

Negative significant correlations were revealed between $\delta^{13}C$ from LN, LS and July precipitations. Yet, correlation coefficients did not remain stable over time for tree-ring parameters from PS and PN (Table 3). Moreover, we found positive significant correlations between TRWI for LS and LN with average VPD of May–August ($r = 0.47$; $P < 0.05$) for the short period of observations from 1959 to 2013. A high correlation ($r = 0.70$; $P < 0.05$) was found for sunshine duration of June and July for $\delta^{13}C$ of LN and TRWI of LN for the period from 2000 to 2013. Significant influences of RH to $\delta^{13}C$ wood of the larch chronologies (LN and LS) were detected. However, RH of June impacted $\delta^{18}O$ of PS, which is not the case for all other species and aspects.

Long-term variability of WUEi, $\delta^{18}O$ and TRW We applied regression analyses to calculate significance of the long-term trends and to find the 'break points' related to changes in the patterns of: intrinsic WUEi and $\delta^{18}O$, the ratio between intercellular CO_2 (c_i) and ambient CO_2 (c_a), and TRW from larch and pine from south- and north-facing aspects (Figure 4). WUEi showed a significant increasing trend since the 1950s for larch from the both aspects ($R^2 = 0.87$; $P < 0.01$) and pine from both aspects ($R^2 = 0.85$; $P < 0.01$) (Figure 4b), respectively. LS and LN reached saturation after 1990 ($R^2 = 0.54$; $P < 0.01$) (Figure 4a), while WUEi for PS and PN continuously increased (Figure 4b). Intrinsic water-use efficiency from LN showed higher values compared with LS, but this difference decreased towards the end of the record (Figure 4a). The opposite development was found for PS and PN for the last 20 years (Figure 4b). We found a significant correlation between WUEi and $\delta^{18}O$ of LN ($R^2 = 0.25$; $P < 0.05$) (Figure 4a). There were no significant

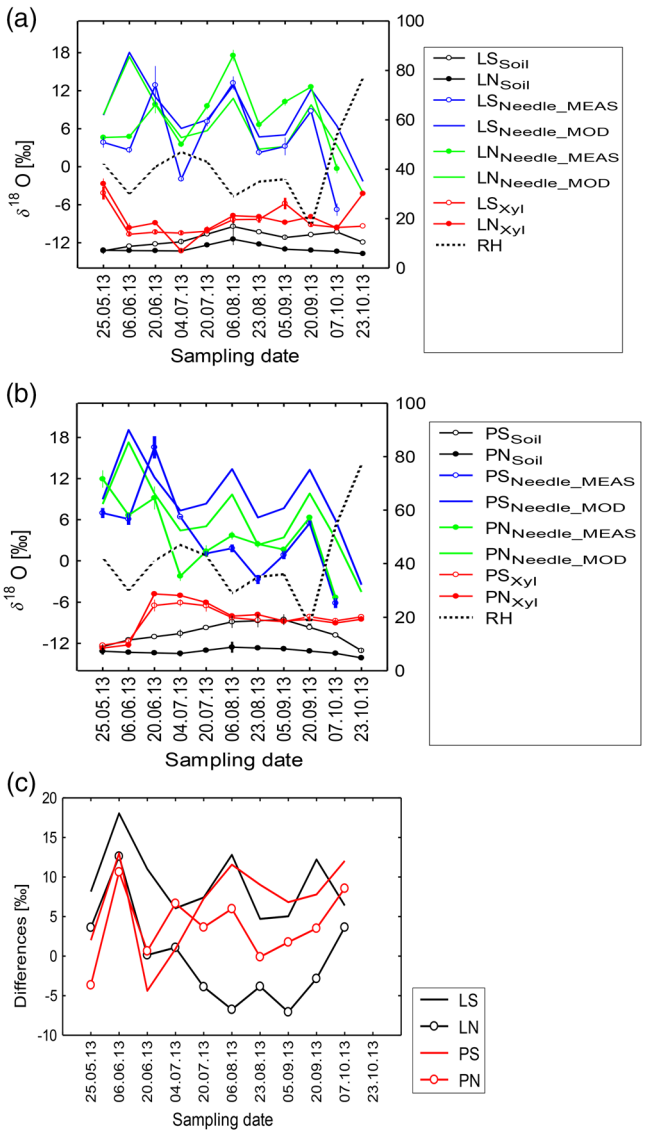

Figure 2. Seasonal course of relative humidity (RH) and measured (MEAS) $\delta^{18}O$ water in (a) larch and (b) pine from south-facing (PS, LS) and north-facing (PN, LN) aspects, respectively in $\delta^{18}O$ xylem ($\delta^{18}O_{Xyl}$), $\delta^{18}O$ needle ($\delta^{18}O_{Needle}$) and $\delta^{18}O$ soil ($\delta^{18}O_{Soil}$) water vs modeled (MOD) $\delta^{18}O$ needle water. The standard error is shown as error bars. (c) Differences between modeled and measured $\delta^{18}O_{Needle}$ water from larch and pine needles form south- and north-facing aspects, respectively.

correlations between $\delta^{18}O$ and WUEi of LS, and WUEi of PN, respectively (Figure 4a and b), while for PS the correlation was weak ($R^2 = 0.04$; $P < 0.05$) (Figure 4b).

The ratio of c_i/c_a showed a slight but significant decline ($R^2 = 0.30$; $P < 0.05$) for pine trees for the period from 1980 to 2013 only (Figure 4d). Tree-ring width for pine (Figure 4f) showed a significant decline after the 1980s ($R^2 = 0.64$; $P < 0.01$), while for larch trees the c_i/c_a ratio decline ($R^2 = 0.24$; $P < 0.05$) ends in the 1980s with a following significant increasing trend of the c_i/c_a ratio ($R^2 = 0.52$; $P < 0.01$) for both aspects (Figure 4c) and with a significant increasing trend ($R^2 = 0.88$; $P < 0.01$) between both aspects for TRW (Figure 4e).

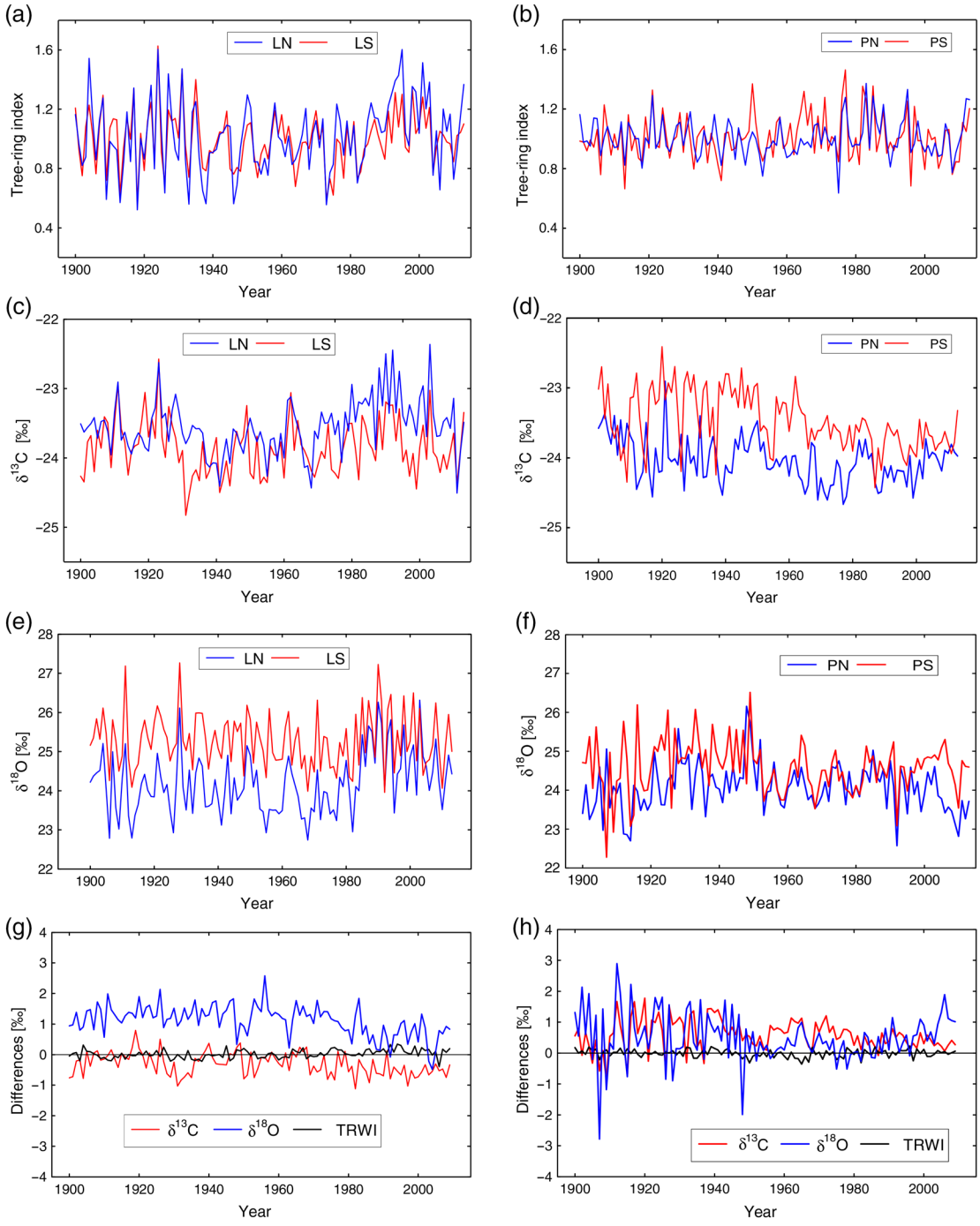

Figure 3. Tree-ring width index (a and b), $\delta^{13}C$ (c and d) and $\delta^{18}O$ (e and f) for larch trees from south- and north-facing aspects (LS and LN) and mountain pine trees from south- and north-facing aspects (PS and PN), respectively. Differences between TRWI, $\delta^{13}C$ and $\delta^{18}O$ in larch (g) and mountain pine (h) were calculated as north-facing aspect subtracted from south-facing aspect. The panels on the left show observations of larch on the south- and north-facing aspects, while the panels on the right show mountain pine on the south- and north-facing aspects.

Discussion

Seasonal differences between species and aspects

We found clear differences in $\delta^{18}O_{Xyl}$ between the two species (Figure 1a and b). $\delta^{18}O_{Xyl}$ pine strongly correlated with $\delta^{18}O_{Pr}$, independent of the sites (Figure 1b), indicating similar $\delta^{18}O$ values of the water source for both aspects and the use of relatively recent precipitation by pine. In contrast, larch $\delta^{18}O_{Xyl}$ negatively correlated with $\delta^{18}O_{Pr}$ for both aspects, which could be explained by deeper rooting depth for larch compared with pine (Figure 1a). The slight enrichment in $\delta^{18}O_{Xyl}$ relative to the $\delta^{18}O_{Pr}$ for PS and PN in spring agrees with findings from Treydte et al. (2014), who suggested integrated water uptake across relatively shallow soil depths. In general, however, our data show

Table 2. Pearson correlation coefficients between TRWI, $\delta^{13}C$ and $\delta^{18}O$ in wood obtained from larch on south- and north-facing aspects (LS and LN) as well as for mountain pine trees from south- and north-facing aspects (PS and PN), respectively. Significant Pearson's correlations are marked in bold at $P < 0.05$.

Species/aspect		LS			LN			PS			PN		
	Parameter	TRWI	$\delta^{13}C$	$\delta^{18}O$	TRWI	$\delta^{13}C$	$\delta^{18}O$	TRWI	$\delta^{13}C$	$\delta^{18}O$	TRWI	$\delta^{13}C$	$\delta^{18}O$
LS	TRWI	1											
	$\delta^{13}C$	0.03	1										
	$\delta^{18}O$	**0.23**	**0.33**	1									
LN	TRWI	**0.81**	–0.04	0.22	1								
	$\delta^{13}C$	**0.26**	**0.56**	**0.36**	0.1	1							
	$\delta^{18}O$	**0.42**	**0.36**	**0.78**	**0.32**	**0.56**	1						
PS	TRWI	**0.31**	0.04	0.08	**0.35**	0.02	0.09	1					
	$\delta^{13}C$	0.02	0.13	**0.26**	0.09	0.01	0.04	–0.04	1				
	$\delta^{18}O$	0.04	0.04	**0.40**	0.05	0.07	**0.30**	0.07	**0.45**	1			
PN	TRWI	**0.28**	–0.01	0.09	**0.25**	0.06	0.07	**0.60**	0.01	0.04	1		
	$\delta^{13}C$	–0.04	0.09	0.11	0.01	0.01	0.08	0.07	0.09	–0.04	0.02	1	
	$\delta^{18}O$	0.02	0.07	**0.44**	–0.02	0.10	**0.38**	–0.04	0.12	**0.23**	0.19	0.20	1

that xylem water is more depleted in ^{18}O than precipitation water. We assume that the warmer it gets, the less surface water is available, causing particularly larch trees to proliferate their roots to deeper soil depths for water acquisition. Our assumptions for larch trees are also confirmed by negative correlations of VPD with $\delta^{18}O_{Xyl}$ for LS and LN (Table 1).

To analyze the differences in needle water $H_2{}^{18}O$ enrichment between the two species and the two aspects we applied the Craig–Gordon model. $\delta^{18}O_{Needle}$ was always enriched in $H_2{}^{18}O$ relative to the source water (Figure 2a and b), yet it varied strongly between the different sampling dates. Although RH is the main driver for the variation in $\delta^{18}O_{Needle}$, we only found a significant relationship between RH and $\delta^{18}O_{Needle}$ for the LN trees. This is consistent with the findings of Roden et al. (2015), who found a low responsiveness to variations in VPD in older (at least 0.5 year old) needles regarding water $H_2{}^{18}O$ enrichment. The fact that LN needle $H_2{}^{18}O$ enrichment correlated significantly with variations in RH (Table 1) could be attributed to the slower needle development, such that the LN needles were not yet as far developed as the LS needles due to the northern exposure. Higher $\delta^{18}O$ values in needle water for LS (Figure 2a) and PS (Figure 2b) could probably indicate warmer/drier climate conditions compared with the colder LN (Figure 2a) and PN aspects (Figure 2b). The seasonal course of RH showed a significant impact only on $\delta^{18}O_{Needle}$ from LN, which confirms our initial finding (Figure 1e).

A larger offset between modeled and measured $\delta^{18}O_{Needle}$ water was found mainly for southern aspects for both species (Figure 2c). These differences indicate model overestimations of $\delta^{18}O_{Needle}$ water enrichment, since the simple Craig–Gordon approach does not take transpiration or stomatal conductance into account. However, during transpiration this water loss is replenished (advection of non-enriched H_2O molecules from the xylem to the location of transpiration) with $H_2{}^{18}O$-depleted source water, leading to a dilution of the $H_2{}^{18}O$ enrichment and thus a decrease in $\delta^{18}O_{Needle}$ water. Thus, leaf water enrichment is diminished, with increasing transpiration. These counteracting mechanisms can be corrected with the Péclet algorithm (Farquhar and Lloyd 1993).

Furthermore, as the Craig–Gordon model does not account for species-specific differences, the leaf water enrichment values ($\delta^{18}O_{Needle}$) were simulated as purely physico-chemical processes, and yield a physico-chemical base line. This model behavior is well known as it does not account for physiological and anatomical properties and assumes steady-state conditions, a status that hardly occurs in nature. Rapid changes in air humidity and temperature as observed in mountainous regions make it hardly possible to reach steady state for ^{18}O leaf water isotopic enrichment, leaf water content (LWC) or water fluxes (E), as these fluctuations impact the leaf water status. Therefore, what we observe are average values, i.e., integrals over time of leaf water ^{18}O enrichment, E and LWC, and even more so for organic compounds.

The differences in deviations between larch and pine from the modeled base line are obvious and are a result of the exposition of the trees, besides physiological and anatomical properties. While larch tends towards broad-leaf physiological traits, pine shows clear conifer characteristics; accordingly, either the Péclet correction would be more suitable, whereas the two pool model might be more suitable for older needles (Roden et al. 2015, Song et al. 2015). However, this is an assumption that needs to be tested in controlled experiments.

Long-term variabilities in TRWI, $\delta^{13}C$ and $\delta^{18}O$

The increasing variability in larch TRWI over 100 years indicates a higher responsiveness towards climatic changes in recent decades. Carbon isotopes and TRWI for larch trees suggest that a decrease in water availability occurred in July, and for PS and PN most likely in May and July (Table 3). Mountain pine trees

Table 3. Pearson's correlation coefficients between TRWI, $\delta^{13}C$ and $\delta^{18}O$ from larch south- and north-facing aspects (LS and LN) and pine from south- and north-facing aspects (PS and PN) and meteorological data (drought index, temperature, precipitation) calculated for the different periods. Significant values are in bold, $P < 0.05$.

Species/ aspect	Parameter	Period	Drought index			Temperature			Precipitation			
			May	July	August	June	July	August	May	July	August	Annual
LS	TRWI	1917–80	**–0.47**	0.19	0.01	**0.25**	0.12	**0.27**	**–0.44**	0.18	0.04	**–0.24**
		1980–2013	–0.22	0.09	0.14	0.23	0.13	0.17	–0.22	0.11	0.12	–0.22
		1917–2013	–0.19	0.04	0.04	0.03	0.14	0.01	–0.18	0.06	0.04	**–0.30**
	$\delta^{13}C$	1917–80	0.17	**–0.35**	**–0.36**	–0.08	0.09	**0.63**	0.15	**–0.35**	**–0.31**	0.00
		1980–2013	0.07	**–0.26**	–0.19	–0.14	0.02	0.21	0.07	**–0.27**	–0.18	0.04
		1917–2013	0.17	**–0.31**	**–0.29**	–0.25	0.08	**0.38**	0.15	**–0.32**	**–0.27**	–0.08
	$\delta^{18}O$	1917–80	0.10	–0.12	–0.17	–0.09	0.17	0.00	0.08	–0.11	–0.18	–0.12
		1980–2013	0.10	**–0.24**	0.11	0.01	**0.45**	**0.38**	0.08	–0.19	0.14	0.17
		1917–2013	0.12	–0.22	–0.01	–0.07	**0.36**	**0.30**	0.10	–0.18	0.01	0.03
LN	TRWI	1917–80	**–0.37**	**0.40**	–0.20	–0.17	**0.33**	0.08	**–0.38**	0.37	–0.19	**–0.32**
		1980–2013	–0.05	0.11	0.16	0.30	0.05	–0.16	–0.08	0.12	0.14	–0.08
		1917–2013	–0.19	0.04	0.04	0.03	0.14	0.01	–0.18	0.06	0.04	**–0.30**
	$\delta^{13}C$	1917–80	–0.13	**–0.41**	0.18	0.18	0.01	**0.51**	–0.07	**–0.45**	0.22	**0.40**
		1980–2013	–0.10	**–0.32**	0.00	–0.02	**0.28**	**0.37**	–0.11	**–0.30**	0.03	0.16
		1917–2013	0.05	**–0.37**	–0.10	–0.19	0.23	**0.49**	0.05	**–0.36**	–0.07	0.00
	$\delta^{18}O$	1917–80	–0.20	0.02	–0.20	**–0.27**	–0.16	0.16	–0.22	–0.01	–0.19	**–0.33**
		1980–2013	0.02	**–0.31**	0.14	0.13	**0.43**	**0.35**	0.00	**–0.27**	0.16	0.12
		1917–2013	0.02	**–0.25**	–0.06	–0.13	**0.27**	**0.39**	–0.01	–0.23	–0.04	–0.14
PS	TRWI	1917–80	**0.37**	–0.17	**0.53**	–0.06	**0.54**	**–0.34**	**0.41**	–0.09	**0.51**	–0.18
		1980–2013	0.20	0.08	–0.02	0.01	–0.05	–0.05	**0.24**	0.08	–0.02	–0.03
		1917–2013	**0.32**	–0.06	0.05	–0.10	0.18	–0.02	**0.36**	–0.03	0.05	–0.16
	$\delta^{13}C$	1917–80	**0.34**	**–0.29**	**0.23**	**0.41**	**0.24**	–0.09	**0.35**	**–0.26**	**0.23**	**0.68**
		1980–2013	0.09	–0.03	0.06	0.06	**0.31**	**0.30**	0.09	–0.01	0.07	0.13
		1917–2013	0.13	–0.06	0.10	0.12	**0.27**	0.20	0.13	–0.04	0.11	**0.23**
	$\delta^{18}O$	1917–80	**0.39**	–0.26	–0.22	–0.01	**0.30**	**0.31**	**0.32**	–0.22	**–0.26**	–0.04
		1980–2013	–0.08	–0.03	0.06	**0.24**	0.22	0.16	–0.05	–0.01	0.07	0.06
		1917–2013	0.05	–0.05	0.05	0.24	0.21	0.03	0.05	–0.03	0.04	0.08
PN	TRWI	1917–80	0.22	–0.22	**0.60**	–0.06	**0.74**	**0.32**	**0.24**	–0.12	**0.57**	0.07
		1980–2013	0.01	0.08	0.20	**0.27**	0.16	–0.03	0.09	0.09	0.18	–0.03
		1917–2013	0.12	–0.02	**0.25**	0.15	**0.32**	–0.04	0.16	0.02	0.23	–0.04
	$\delta^{13}C$	1917–80	**0.38**	**–0.24**	–0.09	**0.49**	0.24	**0.38**	**0.41**	–0.22	–0.07	**0.62**
		1980–2013	–0.22	–0.12	0.03	0.12	**0.28**	0.16	–0.23	–0.09	0.04	0.09
		1917–2013	–0.10	–0.06	0.11	**0.29**	0.19	0.03	–0.08	–0.04	0.11	**0.26**
	$\delta^{18}O$	1917–80	0.21	–0.22	**0.23**	0.15	0.09	**0.44**	0.21	–0.22	0.19	0.12
		1980–2013	0.02	–0.08	**0.44**	0.14	**0.23**	0.20	0.04	–0.06	**0.46**	0.15
		1917–2013	0.07	–0.10	**0.40**	0.16	0.18	0.04	0.09	–0.09	**0.41**	0.16

from both aspects were sensitive to changes of relative humidity during warm months such as June and July. The positive significant correlations between $\delta^{18}O$ for larch with May and July precipitation could be explained by a high VPD. A similar finding was reported by Schollaen et al. (2013), who revealed a positive relationship between $\delta^{18}O$ in tree-ring cellulose and precipitation for dry seasons. Mountain pine trees indicate a developing water shortage during earlier spring only, and show a positive significant relationship with VPD. This is further reflected in an increase in $\delta^{18}O$ enrichment of needle water, which is not the case for larch trees. Streit et al. (2014) reported a positive linear relationship between $\Delta^{18}O$ and VPD for both larch and mountain pine at Stillberg (Davos, Switzerland). The contrasting patterns at our study site (Table 1), e.g., high positive correlations between pine trees and VPD and negative correlations with larch trees, suggest different hydrological conditions, which could be explained by differences in the root development resulting in different water sources for these tree species. For example, Alvarez-Uria and Körner (2007) and Körner (2012) showed that specific root length (i.e., root length produced per unit of dry matter) of pine trees from high-elevation sites is ~35 m g^{-1} compared with larch trees with ~40 m g^{-1}. The root diameter is similar for larch (0.39 mm) and pine (0.38 mm) trees. Moreover, they showed

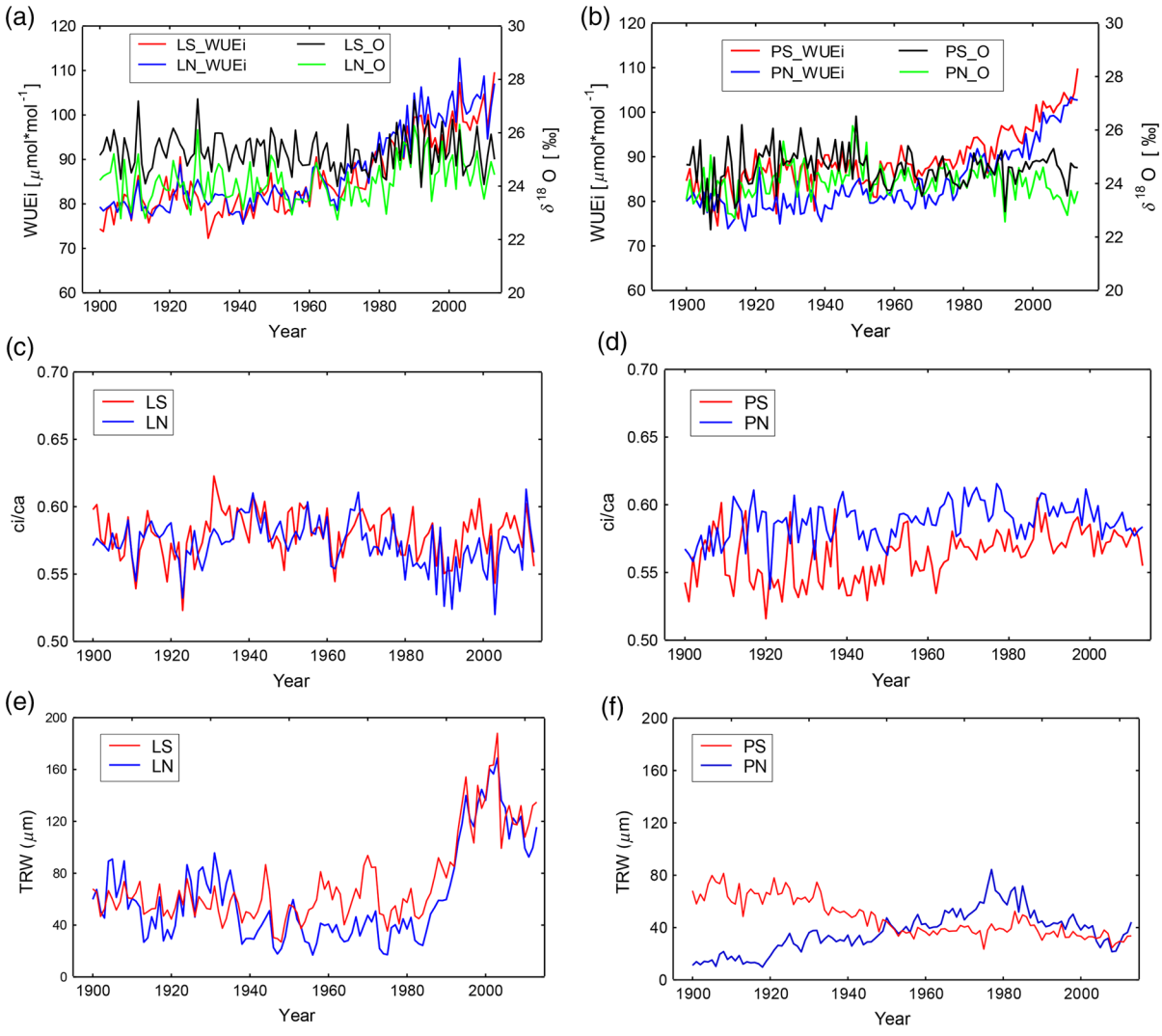

Figure 4. Intrinsic water-use efficiency calculated for LS (red line) and LN (blue line) (a), and PS (red line) and PN (blue line) (b) vs $\delta^{18}O$ wood chronologies for LS (black line) and LN (green line) (a), and PS (black line) and PN (green line) (b), respectively. Ratio of ambient CO_2 (c_a) to intercellular CO_2 (c_i) calculated for LS and LN (c), and PS and PN (d). TRW (raw data) for larch trees (e) from south- and north-facing aspects (LS and LN) and pine trees (f) from south- and north-facing aspects (PS and PN), respectively.

that for a 10 mm diameter root, the attached dry mass to the finest root level is for larch on average 2.3 g and for mountain pine 3.4 g. The results show that the functional rooting depth is a fundamental species-specific and site-specific trait that regulates the whole-tree physiological strategy and thus the isotopic fingerprint in tree rings.

Based on the long-term variabilities in TRWI, $\delta^{13}C$ and $\delta^{18}O$ and based on the short-term variabilities in $\delta^{18}O_{Xyl}$, $\delta^{18}O_{Needle}$ and $\delta^{18}O_{Soil}$ water, we found that the physiological response of mountain pine trees to seasonal changes is different compared with larch trees. Relative humidity and July temperature highly influenced larch trees, while the impact of precipitation becomes more important for pine trees. This indicates that pine trees rather use the soil surface water (Table 1; Figure 1b, e and f), whereas larch trees seem to be able to utilize water from the deeper soil layers (Table 1; Figure 1a, b and c), and most likely can penetrate with their rooting system into rock cracks and access water from deeper ground levels.

Long-term variability of WUEi and $\delta^{18}O$ in wood and TRW

We calculated WUEi for larch (Figure 4a; LN and LS) and mountain pine (Figure 4b; PS and PN). Larch WUEi showed significant increasing trends for LS and LN over time with saturating characteristic for the last 20 years. This is in agreement with increasing tree-ring values (Figure 4e) and increasing trend of c_i/c_a since the 1980s and saturation point over last 20 years for both aspects, which could be explained by the plasticity of larch trees to improving growth conditions, i.e., rapidly increasing CO_2, and non-limiting water supply for larch (deep rooting tree). We found divergent trends between WUEi for PS and PN, and $\delta^{18}O$ during the period from 1993 to 2013 (Figure 4b). The TRW chronology from PN (Figure 4f) indicates more favorable growth

conditions until the 1980s followed by a decline of TRWs. However, this is not the case for TRW from PS, where tree growth was impaired for a long time. According to Scheidegger et al. (2000) decreasing $\delta^{18}O$ in organic matter reflects an increase in g_s. Considering the results above this is not plausible from an eco-physiological point of view. However, it could be the consequence of an impaired stomatal regulation, which is often observed in either senescing or dying plants. Eventually, this will lead to a decoupling of the isotopic signals between needles and tree rings. Pflug et al. (2015) observed a progressive decrease in tree-ring growth and photosynthesis with increasing drought. They found that the amount of carbohydrates became insufficient for tree-ring growth. Thus, the isotopic signal formed in the needles during periods with growth-limiting conditions is no longer stored in the tree rings. What remains are sections of tree rings, which were formed under less limiting, usually more humid conditions during spring and fall, when $\delta^{18}O_{Pr}$ is more depleted than in summer.

Conclusion

Our study showed

(i) Differences occur in the seasonal courses of $\delta^{18}O_{Needle}$, $\delta^{18}O_{Xyl}$ and $\delta^{18}O_{Soil}$ water between species and between aspects. There is a strong and significant coupling of $\delta^{18}O_{Pr}$ and $\delta^{18}O_{Xyl}$ water for mountain pine for both aspects and for larch on the north-facing aspect, which indicates a similar water source used by the trees in the short-term. Yet, RH affected larch from north-facing aspect only. The application of the Craig–Gordon model showed an over-estimation of $\delta^{18}O_{Needle}$ water enrichment due to the high transpiration rate.

(ii) Summer temperatures as well as summer and annual sums of precipitations are important factors for growth of both studied species from both aspects in the SNP. However, mountain pine trees reduced sensitivity to temperature changes, while precipitation changes come to play a more important role for the period from 1980 to 2013.

(iii) Intrinsic water-use efficiency strategies differ between mountain pine and larch trees under recent climatic changes. Since the 1990s WUEi calculated for larch reached saturation, possibly showing an adaptation or limitation to elevated CO_2. However, WUEi calculated for mountain pine trees from the same period continuously increased. Divergent trends between pine WUEi and $\delta^{18}O$ values, and narrow TRWs could be the result of senescence or declining mountain pine trees in the SNP resulting in a decoupling of the isotopic signal between needles and TRW chronology.

(iv) Understanding the eco-physiological constraints on the isotopic composition of $\delta^{13}C$ and $\delta^{18}O$ in tree rings and $\delta^{18}O$ needle water enrichment has important implications for the interpretation of tree-ring isotopes for climate reconstruction and for the study of the impacts of climate change on forests for the two studied species.

Acknowledgments

We are grateful to Ruedi Haller, Thomas Scheurer and Samuel Wiesmann for their help and we would like to acknowledge the research committee of the Swiss National Park for the sampling permission in the protected area. We thank our colleagues from ETH Zurich and Paul Scherrer Institute, who helped with the field sampling and supported us in the laboratory. Special thanks to Lucas Cernusak and the three reviewers for their valuable comments on our manuscript.

Conflict of interest

None declared.

Funding

This work was supported by the Swiss National Science Foundation, Marie-Heim Voegtlin Programme PMPD2-145507 granted to O.V.C and COST-action FP1106 (SBF C12.0093) granted to M.S.

References

Allen CD, Macalady AK, Chenchouni H et al. (2010) A global overview of drought and heat-induced tree mortality reveals emerging climate change risks for forests. For Ecol Manag 259:660–684.

Alvarez-Uria P, Körner C (2007) Low temperature limits of root growth in deciduous and evergreen temperate tree species. Funct Ecol 21:211–218.

Anderegg WRL, Berry JA, Smith DD, Sperry JS, Anderegg LDL, Field CB (2012) The roles of hydraulic and carbon stress in a widespread climate-induced forest die-off. Proc Natl Acad Sci USA 109:233–237.

Barbour MM, Walcroft AS, Farquhar GD (2002) Seasonal variation in $\delta^{13}C$ and $\delta^{18}O$ of cellulose from growth rings of *Pinus radiata*. Plant Cell Environ 25:1483–1499.

Bendel M, Kienast F, Bugmann H, Rigling D (2006*a*) Incidence and distribution of *Heterobasidion* and *Armillaria* and their influence on canopy gap formation in unmanaged mountain pine forests in the Swiss Alps. Eur J Plant Pathol 116:85–93.

Bendel M, Kienast F, Rigling D, Bugmann H (2006*b*) Impact of root-rot pathogens on forest succession in unmanaged *Pinus mugo* stands in the Central Alps. Can J Forest Res 36:2666–2674.

Bottinga Y, Craig H (1968) Oxygen isotope fractionation between CO_2 and water, and the isotopic composition of marine atmospheric CO_2. Earth Planet Sci Lett 5:285–295.

Brang P (1988) Decline of mountain pine (*Pinus mugo* ssp. *uncinata*) stands in the Swiss National Park: a dendrochronological approach. Dendrochronologia 6:151–162.

CH (2011) Swiss climate change scenarios CH2011. C2SM, MeteoSwiss, ETH, NCCR Climate, and OcCC, p 88.

Cherubini P, Fontana G, Rigling D, Dobbertin M, Brang P, Innes JL (2002) Tree-life history prior to death: two fungal root pathogens affect tree-ring growth differently. J Ecol 90:839–850.

Cook ER, Kairiukstis LA (1990) Methods of dendrochronology. In: Cook ER, Kairiukstis LA (eds) Applications in the environmental sciences. Kluwer Academic Publishers, Doredrecht, p 393.

Craig H (1961) Isotopic variations in meteoric waters. Science 133:1702–1703.

Craig H, Gordon LI (1965) Deuterium and oxygen-18 variations in the ocean and the marine atmosphere. In: Tongiogi E (ed) Proc. stable isotopes in oceanographic studies and paleotemperatures. V. Lishi e F., Pisa. pp 9–130.

Dongmann G, Nürnberg HW, Förstel H, Wagener K (1974) On the enrichment of $H_2{}^{18}O$ in the leaves of transpiring plants. Radiat Environ Biophys 11:41–52.

Farquhar GD, Lloyd J (1993) Carbon and oxygen isotope effects in the exchange of carbon dioxide between terrestrial plants and the atmosphere. In: Ehleringer JR, Hall AE, Farquhar GD (eds) Stable isotopes and plant carbon-water relations. Academic Press, San Diego, CA, pp 47–70.

Farquhar GD, Sharkey TD (1982) Stomatal conductance and photosynthesis. Annu Rev Plant Physiol 33:317–345.

Farquhar GD, Ehleringer JR, Hubick KT (1989) Carbon isotope discrimination and photosynthesis. Annu Rev Plant Physiol Plant Mol Biol 40:503–537.

Förstel H, Hützen H (1983) $^{18}O/^{16}O$ ratio of water in a local ecosystem as a basis of climate record. In: Proceedings IAEA, Paleoclimates and paleowaters. A collection of environmental isotope studies. IAEA, Vienna, Austria, pp 67–81.

Holmes RL (1983) Computer-assisted quality control in tree-ring dating and measurement. Tree-Ring Bull 43:69–78.

Körner Ch (2012) Alpine tree lines. Springer, Basel.

Klein T (2015) Drought-induced tree mortality: from discrete observations to comprehensive research. Tree Physiol 35:225–228.

McCarroll D, Loader NJ (2004) Stable isotopes in tree rings. Quat Sci Rev 23:771–801.

Pachauri RK, Meyer LA et al. (2014) Climate change 2014: synthesis report. In: Pachauri RK, Meyer LA (eds) Contribution of working groups I, II and III to the fifth assessment report of the intergovernmental panel on climate change. IPCC, Geneva, Switzerland, p 151.

Pflug EE, Siegwolf R, Buchmann N, Dobbertin M, Kuster TM, Günthardt-Goerg MS, Arend M (2015) Growth cessation uncouples isotopic signals in leaves and tree rings of drought-exposed oak trees. Tree Physiol 35:1095–1105.

Roden JS, Ehleringer JR (1999) Observations of hydrogen and oxygen isotopes in leaf water confirm the Craig-Gordon model under wide-ranging environmental conditions. Plant Physiol 120:1165–1173.

Roden J, Kahmen A, Buchmann N, Siegwolf R (2015) The enigma of effective path length for ^{18}O enrichment in leaf water of conifers. Plant Cell Environ 38:2551–2565.

Roden JS, Lin G, Ehleringer JR (2000) A mechanistic model for interpretation of hydrogen and oxygen isotope ratios in tree-ring cellulose. Geochim Cosmochim Acta 64:21–35.

Sala A, Piper F, Hoch G (2010) Physiological mechanisms of drought-induced tree mortality are far from being resolved. New Phytol 186:274–281.

Saurer M, Aellen K, Siegwolf R (1997) Correlating $\delta^{13}C$ and $\delta^{18}O$ in cellulose of trees. Plant Cell Environ 20:1543–1550.

Saurer M, Spahni R, Frank DC et al. (2014) Spatial variability and temporal trends in water-use efficiency of European forests. Glob Change Biol 20:3700–3712.

Scheidegger Y, Saurer M, Bahn M, Siegwolf R (2000) Linking stable oxygen and carbon isotopes with stomatal conductance and photosynthetic capacity: a conceptual model. Oecologia 125:350–357.

Schollaen K, Heinrich I, Neuwirth B, Krusic PJ, D'Arrigo RD, Karyanto O, Helle G (2013) Multiple tree-ring chronologies (ring width, $\delta^{13}C$ and $\delta^{18}O$) reveal dry and rainy season signals of rainfall in Indonesia. Quat Sci Rev 73:170–181.

Sidorova OV, Siegwolf RTW, Saurer M, Naurzbaev MM, Vaganov EA (2008) Isotopic composition ($\delta^{13}C$, $\delta^{18}O$) in wood and cellulose of Siberian larch trees for early Medieval and recent periods. J Geophys Res Biogeosc 113:1–13.

Sidorova OV, Siegwolf RTW, Saurer M, Shashkin AV, Knorre AA, Proklushkin AS, Vaganov EA, Kirdyanov AV (2009) Do centennial tree-ring and stable isotope trends of *Larix gmelinii* (Rupr.) Rupr. indicate increasing water shortage in the Siberian north? Oecologia 161:825–835.

Solar J (2013) Effect of climate change on mountain pine distribution in western Tatra Mountains. In: Singh BR (ed), Climate change-realities, impacts over ice cap, sea level and risks. Chapter 18. doi:10.54772/54724.

Song X, Loucos KE, Simonin KA, Farquhar GD, Barbour MM (2015) Measurements of transpiration isotopologues and leaf water to assess enrichment models in cotton. New Phytol 206:637–646.

Streit K, Siegwolf RTW, Hagerdon F, Schaub M, Buchmann N (2014) Lack of photosynthetic or stomatal regulation after 9 years of elevated $[CO_2]$ and 4 years of soil warming in two conifer species at the alpine treeline. Plant Cell Environ 37:315–326.

Thornthwaite CW (1948) An approach toward a rational classification of climate. Geogr Rev 38:55–94.

Treydte K, Boda S, Graf Pannatier E et al. (2014) Seasonal transfer of oxygen isotopes from precipitation and soil to the tree ring: source water versus needle water enrichment. New Phytol 202:772–783.

Yakir D (1998) Oxygen-18 of leaf water: a crossroad for plants-associated isotopic signals. In: Griffiths H (ed) Stable isotopes and the integration of biological, ecological and geochemical processes. Bios, Oxford, pp 147–168.

Wigley TML, Briffa KR, Jones PD (1984) On the average value of correlated time series, with applications in dendroclimatology and hydrometeorology. J Clim Appl Met 23:201–213.

Woodley EJ, Loader NJ, McCaroll D, Young GHF, Robertson I, Heaton THE, Gagen MH, Warham JO (2012) High-temperature pyrolysis/gas chromatography/isotope ratio mass spectrometry: simultaneous measurement of the stable isotopes of oxygen and carbon in cellulose. Rapid Commun Mass Spectrom 26:109–114.